Genetic surveillance of *Plasmodium falciparum* populations following treatment policy revisions in the Greater Mekong Subregion

Varanya Wasakul[1], Tess D Verschuuren[1], Nguyen Thuy-Nhien[2], Ethan Booth[1], Huynh Hong Quang[3], Ngo Duc Thang[4], Keobouphaphone Chindavongsa[5], Siv Sovannaroth[6], Virasak Banouvong[5], Viengphone Sengsavath[5], Mayfong Mayxay[7,8,9], Nguyen Thi Kim Tuyen[2], Vo Ngoc Lam Phuong[2], Pham Duc Trung[2], Sónia Gonçalves[10], Soun Chen[6], Sonexay Phalivong[7], Saiamphone Xayvanghang[7], Supaporn Mahaphontrakoon[1], Richard D Pearson[10], Paul N Newton[7,9], Richard J Maude[1,9,11], Elizabeth A Ashley[7,9], Cristina V Ariani[10], Victoria J Simpson[10], Nicholas P Day[1,9], Arjen M Dondorp[1,9], Olivo Miotto[1,9*]

[1]Mahidol Oxford Tropical Medicine Research Unit, Faculty of Tropical Medicine, Mahidol University, Bangkok, Thailand
[2]Oxford University Clinical Research Unit, Ho Chi Minh City, Vietnam
[3]Institute of Malariology, Parasitology and Entomology, Quy Nhon, Vietnam
[4]National Institute of Malariology, Parasitology and Entomology, Hanoi, Vietnam
[5]Centre for Malariology, Parasitology, and Entomology, Vientiane, Lao PDR
[6]National Center for Parasitology, Entomology and Malaria Control, Phnom Penh, Cambodia
[7]Lao-Oxford-Mahosot Hospital-Wellcome Trust Research Unit, Microbiology Laboratory, Mahosot Hospital, Vientiane, Lao PDR
[8]Institute of Research and Education Development, University of Health Sciences, Ministry of Health, Vientiane, Lao PDR
[9]Centre for Tropical Medicine and Global Health, Nuffield Department of Medicine, University of Oxford, Oxford, UK
[10]Wellcome Sanger Institute, Hinxton, UK
[11]The Open University, Milton Keynes, UK

* Corresponding author, e-mail: olivo@tropmedres.ac

ABSTRACT

Genetic surveillance of *Plasmodium falciparum* (*Pf*) can track antimalarial-resistant strains, to inform decision-making by National Malaria Control Programmes (NMCPs). The GenRe-Mekong project prospectively collected 5,982 samples in the Greater Mekong Subregion (GMS) between 2017 and 2022, genotyping drug resistance markers, and barcodes that recapitulate genetic variation. Genotypes were analysed with the grcMalaria R package, designed to translate genetic epidemiology data into actionable visual information. Since 2020, *Pf* incidences decreased rapidly, accompanied by a decline of dihydroartemisinin-piperaquine (DHA-PPQ) resistant lineages, previously dominant in the eastern GMS. The frequency of *plasmepsin2/3* amplifications, conferring piperaquine resistance, dropped from 62% in 2017-2019 to 2% in 2022, coinciding with a switch in frontline therapy in Cambodia, Thailand, and Vietnam. While regional artemisinin resistance levels remained high, no evidence of emerging mefloquine resistance was found. Routine genetic surveillance proved valuable in monitoring rapid parasite population changes in response to public health interventions, providing actionable information for NMCPs.

Key words: malaria, *Plasmodium falciparum*, genetic surveillance, drug resistance, genetic epidemiology, Greater Mekong Subregion.

42 **INTRODUCTION**

43 *Plasmodium falciparum* (*Pf*), a causative agent of malaria, is responsible for more than 500,000 deaths
44 per year, mainly in young African children.[1] Since the turn of the century, mortality has reduced, partly
45 thanks to the availability of efficacious artemisinin-based combination therapies (ACTs), currently the
46 first-line treatment in most endemic countries. However, parasites resistant to artemisinin and/or one
47 of its ACT partner drugs have been reported in several regions, and have been circulating in the
48 Greater Mekong Subregion (GMS) for over 15 years.[2-8] One of the tools used to counteract the spread
49 of drug resistance is genetic surveillance,[9,10] which can be used to map molecular markers of resistance
50 and conduct population-level analyses. The resulting information provides public health authorities
51 with actionable knowledge that supports malaria control and elimination use cases, such as selecting
52 antimalarial drug policies, monitoring drug resistance, and responding to outbreaks.[11]

53 One of the most critical priorities for National Malaria Control Programmes (NMCPs) in the GMS is to
54 monitor and respond to population-level changes in antimalarial drug resistance. The spread of
55 multidrug-resistant KEL1/PLA1 strains in the eastern GMS since 2008, resulted to widespread failures
56 of dihydroartemisinin-piperaquine (DHA-PPQ), which was the frontline treatment in Cambodia,
57 Thailand and Vietnam.[12,13] As recommended by the World Health Organization (WHO), NMCPs in these
58 countries switched to alternative first-line ACTs once DHA-PPQ efficacy fell below the recommended
59 threshold of 90%:[14,15] Cambodia adopted a phased re-introduction of artesunate-mefloquine (AS-MQ)
60 in 2017,[16-19] while five provinces of Vietnam and two provinces of north-eastern Thailand adopted
61 artesunate-pyronaridine (AS-PYR) in 2020.[18-23] The Lao People's Democratic Republic (also known as
62 Lao PDR or Laos) continued the use of artemether-lumefantrine (AL), since its efficacy remained
63 satisfactory.[19,22,24]

64 The GenRe-Mekong project was established to conduct malaria genetic surveillance in partnership
65 with NMCPs and local researchers in the GMS.[9] Parasitized dried blood spots (DBS) are collected from
66 patients presenting at one of the dozens of partner public health facilities which form the sampling

67 framework. DBS are then processed using the SpotMalaria amplicon sequencing platform to extract
68 extensive genetic profiles known as Genetic Report Cards (GRC), which in turn are analysed at
69 population level to produce reports that are returned to NMCPs. SpotMalaria targets specific
70 genotypes associated with antimalarial resistance (Supplementary Table 1),[9] and profiles each sample
71 with a set of polymorphisms- known as a genetic barcode- that is informative of genetic structure and
72 diversity in *Pf* populations.[9,25-27] To accelerate the integration of the genetic surveillance data into
73 public health decision-making processes, NMCPs are supported with technical, genetic, and domain
74 knowledge, to assist with data interpretation. An essential informatic tool used in these analyses is
75 the grcMalaria library, developed by the GenRe-Mekong project and presented in this article. This R
76 package turns genomic data into meaningful graphical visualizations that support NMCP activities,
77 such as geographical maps of malaria resistance prevalence, diversity and relatedness. The tool is easy
78 to use, requiring very few lines of coding, and returns results rapidly as image and spreadsheet files,
79 making geospatial analyses accessible to a wide range of users with different backgrounds.

80 We presented early results from the GenRe-Mekong project in a previous publication.[9] Here, we
81 provide an update, describing changes in antimalarial drug resistance epidemiology in the GMS, based
82 on an analysis of 5,982 *Pf* dried blood spot samples collected by GenRe-Mekong from symptomatic
83 patients in Cambodia, Laos, and Vietnam between 2017 and 2022, a period of time during which
84 several NMCPs changed their malaria frontline treatment policies.

85 METHODS

86 The procedures, operations and technical aspects of the GenRe-Mekong project were detailed in a
87 previous publication;[9] here, we briefly summarize the salient points.

88 Sample collection.

89 Samples were collected from symptomatic patients of all ages who had been confirmed positive for
90 *Pf* by positive rapid diagnostic test or blood smear microscopy. Two or three 20 µL DBS were collected

91 on filter paper by finger-prick, labelled with a unique anonymous identifier, and stored in plastic bags
92 with silica gel before being shipped to the laboratories. In Laos, samples were collected in 5 provinces
93 by the Center for Malariology, Parasitology, and Entomology (CMPE) and the Lao-Oxford-Mahosot
94 Hospital-Wellcome Trust Research Unit (LOMWRU); in Vietnam, sampling was carried out from 11
95 provinces by the Institute of Malariology Parasitology and Entomology Quy Nhon (IMPE-QN), the
96 National Institute of Malariology, Parasitology and Entomology (NIMPE) and the Oxford University
97 Clinical Research Unit (OUCRU); and in Cambodia, samples were collected in 5 provinces by the
98 National Center for Parasitology, Entomology and Malaria Control (CNM) (Supplementary Table 2). In
99 each country, the samples networks were planned by the NMCP, who selected and enrolled sites in
100 collaboration with the relevant provincial health authorities. Staff training was delivered jointly by
101 NMCP officers, provincial health officers and GenRe-Mekong staff. Ethical approvals were obtained
102 both from ethics committees in the country of collection, and from the Oxford Tropical Research Ethics
103 Committee (OxTREC), as previously detailed.[9]

104 **Sample genotyping**

105 DNA was extracted from DBS samples and processed using the SpotMalaria v2 amplicon sequencing
106 protocol as previously detailed.[9] Processing took place in GenRe-Mekong partner laboratories at
107 OUCRU, Ho Chi Minh City, Vietnam; or at the Wellcome Sanger Institute (WSI), Hinxton, UK.
108 Supplementary amplification genotyping by qPCR was carried out by OUCRU. The data from
109 sequencing and qPCR were subsequently used to call genotypes for a standardized set of genotypes,
110 gene amplifications and haplotypes associated with resistance to several antimalarials; to construct
111 genetic barcodes consisting of 101 SNP selected for their ability to differentiate populations and their
112 power to recapitulate genetic distance; and to predict the drug resistance status of each sample.
113 Details of the genotyping pipeline and procedures are given in the Supplementary Methods; a list of
114 the drug resistance-related variants genotyped is provided in Supplementary Table 1.

Data analysis and visualisation

To analyse and visualise data from the GRC, we used the grcMalaria package (version 2.0.0) running on R (version 4.2.3).[28] The GRC format requires structured geographical data, which is achieved by linking study locations to administrative divisions from GADM (Database of Global Administrative Areas) [29], a global catalogue of administrative divisions and their coordinates. The grcMalaria package processes standardised genetic surveillance data in the form of a GRC data file, a Microsoft Excel spreadsheet formatted according to the GenRe-Mekong GRC Data Dictionary (https://github.com/GenRe-Mekong/Documents/tree/main/GRC-DataDictionary). The grcMalaria package is not limited to analysing GMS surveillance data presented in this study but are capable of generating maps across different geographical regions using data in the GRC format, such as the global dataset from the MalariaGEN Pf7.[30]

Dedicated functions generate genetic epidemiology maps (including sample distribution, mutation prevalence, and drug resistance maps) and their associated data, which are delivered as image and spreadsheet files. Geographical structuring supports the aggregation of data at different levels of geographical granularity. In all analyses presented here, we aggregated samples at provincial level (First-level Administrative Division). To analyse *Pf* population changes over time, we partitioned our sample set into three periods (2017-2019, 2020-2021, 2022) characterized by different epidemiological scenarios. Sample distributions were mapped using the grcMalaria `mapSampleCounts` function. Malaria prevalence was calculated as the proportion of confirmed *Pf* cases reported to WHO over total number of tested cases.[31-33] To visualize the frequency of parasites resistant to a given antimalarial, we estimated resistance prevalence using the grcMalaria function `mapDrugResistancePrevalence`, which calculates the proportion of samples predicted as resistant, disregarding samples whose drug-resistant status could not be predicted (e.g. mixed infections and low-quality samples). Pie charts, representing allele proportions of drug-resistant markers by administrative division, were generated using the grcMalaria function `mapAlleleProportions`. Allele proportions at a given position were calculated by dividing the number of samples carrying each allele

141 by the total number of samples in the administrative division, disregarding samples carrying multiple
142 alleles and those missing a genotype at that position.

143 Seven loci of the chloroquine resistance transporter (*crt*) gene are associated with piperaquine
144 resistance (PPQ-R).[34] Four of these loci, including T93S, H97Y, I218F, G353V, were genotyped in the
145 SpotMalaria GRC using amplicon sequencing. Of the 5,982 samples presented in the manuscript, 3,066
146 had available genotypes at these positions. To obtain the remaining PPQ-R associated *crt* mutations,
147 we genotyped the relevant positions using whole-genome sequencing data, available for a large
148 subset of samples (n=1581), thus identifying additional genotypes at *crt* F145I and M343L. Due to the
149 technical complexity of *crt* genotyping, a proportion of samples yielded incomplete or missing
150 genotype data. Samples lacking genotype data at any of these loci were excluded from the frequency
151 calculation. In our sample set, no genetic variations were detected at position 350 of the *crt* gene, and
152 therefore we reported no analysis results for the WHO-listed mutation C350R.

153 Graphs were produced either by Microsoft Excel or by the R ggplot2 (version 3.5.1) library; [35] error
154 bars and shaded areas representing 95% confidence intervals were calculated using Wilson Interval
155 with corrections (BinomCI; DescTools R package version 0.99.54).[36]

156 **Statistics**

157 A Cochran-Armitage trend test was conducted to evaluate trends in the proportion of resistant
158 parasites across different periods (CochranArmitageTest; DescTools R package version 0.99.54).
159 Bonferroni post-hoc analyses between group pairs were performed to adjust for the increased risk of
160 Type I errors. Segmented regression analysis was applied to evaluate the impact of two policy changes
161 (frontline ACT switch and COVID-19 movement restrictions) on malaria prevalence and frequencies of
162 *pm23* amplifications over time. Breakpoints corresponding to each intervention were identified using
163 the `segmented` package in R, allowing estimation of shifts in trend before and after each intervention
164 while accounting for time-dependent effects. Where segmented regression was not applicable, due
165 to the absence of policy changes, linear regression was applied to assess general trends over time.

166 Spearman's rank correlation coefficient was used to assess relationship between non-normally
167 distributed malaria prevalence and PPQ-R frequencies (corr.test; stats R package). Logistic regression
168 with *kelch13* alleles as the dependent variable was used to evaluate association with *mdr1* haplotypes
169 (glm; stats R package).

170 **Analysis of highly related parasites**

171 Clusters of highly related parasites were identified based on pairwise genetic barcode similarity s,
172 obtained from the pairwise genetic distance d where $s=(1-d)$. Pairwise genetic distances between
173 two samples were computed by comparing the alleles carried by the two samples at each of the
174 barcoding SNPs, as previously described.[37] To minimize the influence of missingness on genetic
175 distance estimations, we only included high-quality samples (<25% barcode genotype missingness),
176 and high-quality barcoding SNPs (<20% samples with missing genotype), and applied a simple
177 imputation method at positions where the genotype was missing. At each missing genotype, the
178 imputation method used the pairwise genetic distance matrix to identified the 100 samples closest to
179 the sample being imputed, and assigned the most common allele observed in this group as the
180 imputed allele. Cluster detection was performed by the grcMalaria `findClusters` function, which
181 constructs a graph connecting sample pairs with s greater than a specified minimal threshold $s_{\min}$, and
182 then applies the Louvain multilevel community detection algorithm.[38] We specified a genetic similarity
183 threshold of 95% ($s_{\min}$=0.95) to cluster parasites with essentially identical genetic barcodes, while
184 allowing for low levels of genotyping error; clusters with fewer than 10 members were disregarded.
185 The proportion of the most prevalent clusters were visualised as pie charts, generated using the
186 grcMalaria `mapClusterSharing` function.

187 **Data availability**

188 This paper uses a subset of GenRe-Mekong data, which includes all samples collected by the project
189 during routine surveillance in the eastern GMS. The GenRe-Mekong project has made all genetic data
190 openly available at https://github.com/GenRe-Mekong/Data, including: the full GenRe-Mekong

191 dataset, containing 13,647 samples from eight countries; a subset that includes 5,982 *Pf* samples from
192 the present analysis; and a global dataset containing 16,203 high quality samples, derived from whole-
193 genome sequencing data from the MalariaGEN Pf7 data resource.[30] The datasets are provided in the
194 GRC format, along with a data dictionary for converting third-party data into GRC format for
195 compatibility with the grcMalaria library. Links to source code for the grcMalaria R package can be
196 found at https://github.com/malariagen/grcMalaria, and a comprehensive guide detailing its
197 functions is available at https://genremekong.org/tools/grcmalaria-r-package-user-guide. For quick
198 exploration of published data, an interactive web tool built on the grcMalaria R package is available at
199 https://genremekong.org/tools/grc-mapper. Sequence data for this study has been deposited in the
200 European Nucleotide Archive at EMBL-EBI under accession number PRJEB85801.

201 **Role of the funding source**

202 The funders of the study had no role in study design, data collection, data analysis, data interpretation,
203 or writing of the report.

204 **RESULTS**

205 Between January 2017 and December 2022, GenRe-Mekong collected and processed a total of 5,982
206 *Pf* samples from 21 provinces in three countries (Figure 1b, Supplementary Figure 1). In Vietnam, the
207 project processed 3,340 samples in 2017-2022 (32.7% of WHO-reported *Pf* infections); in Laos, it
208 processed 2,400 samples over the same period (16.2%); while in Cambodia, collections took place
209 between July 2020 and December 2022, producing 242 samples (15.5% of the WHO-reported
210 infections in the country) (Supplementary Figure 2).[31-33] A rapid decline in national *Pf* prevalence
211 occurred sequentially across the three neighbouring countries: first in Cambodia starting in 2018, then
212 in Laos from 2019, and finally in Vietnam from 2020 (Figure 1a). This decline in prevalence reflected a
213 decrease in the number of confirmed cases rather than a decline in the number of tests
214 (Supplementary Figure 3). The longitudinal prevalence trend, as reported by WHO,[31-33] has a strong

215 correspondence with the number of samples collected by the project in Laos and Vietnam, indicating
216 that routine surveillance data can serve as an indicator of *Pf* prevalence in these countries (Figure 1a).
217 As the number of cases declined over time, *Pf* populations became more spatially patchy. By 2022,
218 the majority of samples were concentrated in one province in each country: Attapeu in Laos, Gia Lai
219 in Vietnam, and Pursat in Cambodia (Supplementary Table 2); these provinces had consistently
220 exhibited the highest incidence within their respective countries in previous years. Lack of coverage
221 in certain provinces towards the end of our sampling period reflects underlying epidemiological trends
222 rather than a lack of collection effort: although sampling sites across the whole region were engaged,
223 the marked reduction in *Pf* cases led to some provinces not collecting any samples in the final period.

224 Given this evolution of the *Pf* epidemiological landscape, we opted to conduct longitudinal analyses
225 by partitioning our sample set into three time periods (2017–2019, 2020–2021, and 2022), which
226 reflect different epidemiological scenarios. Specifically, the period from 2020–2021 was a unique
227 phase characterized by policy changes and major external events (e.g., pandemic-related movement
228 restrictions), which differentiates it from both the earlier years and the year 2022. By separating these
229 three periods, we sought to capture and highlight temporal trends more effectively, and assess how
230 change factors have influenced *Pf* epidemiology.

231 **DHA-PPQ resistance decline after changes in first-line treatments**

232 We tracked the spread of DHA-PPQ resistant strains, KEL1/PLA1, by mapping the frequency of two key
233 markers: *pm23* amplifications conferring resistance to piperaquine (PPQ-R) and mutations in *kelch13*
234 gene associated with resistance to artemisinin (ART-R) as listed by the WHO (Supplementary Table
235 1).[34] In the 2017-2019 period, 62% (1,957/3,132) of all collected samples were predicted to be
236 resistant to DHA-PPQ, as they carried both markers (Figure 2a). Prior to that period, DHA-PPQ was
237 used as frontline treatment for uncomplicated malaria in Cambodia, Thailand and Vietnam, which led
238 to cross-border spread of the KEL1/PLA1 strain, resistant to both ACT components, across large areas
239 of the eastern GMS.[13] This strain also spread into the southern Lao provinces of Attapeu and

240 Champasak, where it introduced high levels of DHA-PPQ resistance, despite DHA-PPQ never being
241 selected as a national treatment.[9,37] Starting in 2017, Cambodia gradually switched its frontline
242 treatment from DHA-PPQ to AS-MQ,[17-19,22] while Thailand and Vietnam switched from DHA-PPQ to
243 other ACTs by 2020.[18,19,22,23] Following these changes, regional levels of DHA-PPQ predicted resistance
244 fell steeply, from 63% (1957/3132) to 30% (204/690) in 2020-2021, and 1% (2/278) in 2022 ($Z = -23.9$,
245 $p<0.001$) (Figure 2a). This was underpinned by a decline in predicted PPQ-R, dropping to 31%
246 (228/737) in 2020-2021, and 2% (5/316) in 2022 ($Z = -24.5$, $p <0.001$) (Figure 3a, Supplementary Figure
247 4).

248 Regional *Pf* prevalence shows a highly significant positive correlation with levels of predicted PPQ-R
249 estimated from the proportions of *pm23* amplifications ($R = 0.64$, $p <0.001$), where periods of lower
250 prevalence were generally characterized by lower PPQ-R proportions, suggesting that switching away
251 from the use of DHA-PPQ as the frontline ACT may have had an impact on prevalence (Supplementary
252 Figure 5). However, we cannot exclude other factors that may have contributed to the decline in the
253 number of cases: in particular, the COVID-19 pandemic resulted in travel and trade restrictions that
254 may have affected the transmission and spread of malaria parasites. To tease apart the impact of
255 these two factors, we applied segmented regression to analyze shifts in observable trends at each
256 intervention point; this analysis could only be conducted in Vietnam, where our data supported trend
257 analyses before and after the two interventions. Following the change of frontline ACT, a significant
258 reduction in prevalence was observed ($\beta = -0.1069$, $p = 0.017$), reversing the upward trend to a
259 negative slope. Although the pandemic-related lockdown policy also shifted the trajectory from
260 positive to negative, its immediate impact on prevalence was more modest and statistically non-
261 significant ($\beta = -0.0526$, $p = 0.111$). These results suggest that, although both interventions impacted
262 the decline in prevalence in Vietnam with robust explanatory power ($R^2 \approx 0.70$), the switch of frontline
263 ACT had a more pronounced and statistically significant impact on reduction (Supplementary Figure
264 6c). Data from Vietnam also revealed a strong correlation between predicted PPQ-R prevalence–
265 measured by *pm23* amplification–and changes in first-line treatment policy. Following the

266 replacement of DHA-PPQ with AS-PYR in five endemic Vietnamese provinces, we observed a reduction
267 in *Pf* prevalence and parasites with *pm23* amplifications within three months, ultimately leading to
268 the complete disappearance of PPQ-R parasites within 18 months (Figure 4, Supplementary Figure 6c).
269 The effect of frontline ACT changes could not be assessed in Cambodia, since their policy change took
270 place near the beginning of our study; Laos did not change its treatment policy during this period
271 (Supplementary Figure 6a, b). In both of these countries, lockdown restrictions during the pandemic
272 showed no significant effect on prevalence, nor on PPQ-R decline (all $p > 0.05$).

273 In addition to *pm23* amplifications, seven *crt* mutations have been associated with reduced
274 susceptibility to piperaquine, either *in vivo* or *in vitro*.[34] To confirm the negative trend of PPQ-R
275 frequency in the region, we analysed the frequencies of these *crt* mutations, to investigate whether
276 they are present in parasites lacking the *pm23* amplification marker, and therefore predicted to be
277 sensitive to piperaquine. One associated mutation (C350R) was completely absent from our sample
278 set, while the remaining six mutations circulated at very low frequencies throughout the study period
279 (Supplementary Figure 7 and 8). No increase in the regional prevalence of these *crt* mutation was
280 observed as *pm23* amplifications decreased in frequency. Rather, the frequencies of the two most
281 common mutations (I218F and T93S) declined in parallel with those of the *pm23*. Moreover, *crt*
282 mutations were significantly more likely to be detected in the presence of *pm23* amplifications
283 ($\chi^2=245.2$, $p < 0.001$), suggesting these resistance markers typically co-occur rather than circulate
284 independently (Supplementary Figure 9). The only exception was the H97Y mutation in Cambodia,
285 which occurred more frequently in samples without *pm23* amplification; however, the declining trend
286 and low prevalence of H97Y (<10% frequency in 2022) are consistent with the waning of PPQ-R
287 (Supplementary Figure 10). The concordant evidence from multiple validated molecular markers-
288 *pm23* amplifications and *crt* mutations- provides support for a regional decline in PPQ-R prevalence
289 during this study period.

290 **Resistance to other antimalarials**

291 ART-R levels remained high throughout the period analysed (Figure 3), except in some provinces at
292 the periphery of the endemic region (Savannakhet in Laos, Quang Tri and Ninh Thuan in Vietnam),
293 where most parasites remained susceptible to both artemisinin and piperaquine (Figure 2b,
294 Supplementary Figure 4), suggesting that local parasite populations were isolated from the spread of
295 DHA-PPQ resistant strains in the eastern GMS. Predicted mefloquine resistance (determined by
296 detection of amplifications of the *mdr1* gene[39]) remained low in the region across the study periods
297 (Figure 3, Supplementary Figure 11), even after Cambodia adopted AS-MQ as frontline therapy in
298 2017;[17] in 2022, we detected no samples with an *mdr1* amplification. Markers of resistance to the
299 historical drugs chloroquine, sulfadoxine and pyrimethamine remained high across the region
300 throughout the study period (Figure 3, Supplementary Figure 12).

301 **Distribution of *kelch13* allele variants across fragmented populations**

302 It has been shown that ART-R strains in the eastern GMS originated from multiple founder populations
303 carrying different *kelch13* alleles.[40,41] Parasite strains carrying *kelch13* haplotypes inherited from those
304 early resistant populations persisted over time,[37] even though their geographical distribution and
305 prevalence often changed (Figure 5). In 2017-2019, the majority of ART-R parasites in the eastern GMS
306 carried the *kelch13* C580Y mutation (98%, 2,482/2,539), and 79% of these mutants (1,957/2,482) were
307 classified as KEL1/PLA1 (possessing both *kelch13* C580Y and *pm23* amplification) (Supplementary
308 Figure 13). However, since 2020 the dominance of KEL1/PLA1 waned, and other *kelch13* variants,
309 previously circulating at low frequency, expanded in the region. In the western provinces of Cambodia,
310 *kelch13* Y493H increased in frequency, and eventually dominated the population in Pursat province in
311 2022 (Figure 5, Supplementary Table 3). In Laos, *kelch13* R539T mutants expanded in 2020-2021 in
312 Attapeu and Champasak provinces, causing an outbreak,[37] and subsequently subsided in 2022 to be
313 replaced by parasites possessing the *kelch13* C580Y mutation without *pm23* amplification in Attapeu.
314 In Vietnam, C580Y remained the dominant *kelch13* variant. We observed that the presence of these

315 ART-R *kelch13* alleles was strongly associated with *mdr1* haplotype NFD, characterized by the Y184F
316 mutation (β = 3.44, p<0.001), whereas wild-type *kelch13* parasites mostly carried the *mdr1* haplotypes
317 NYD (wild-type) and YYD (β = -5.14/-6.81, p<0.001) (Supplementary Figure 14).

318 **Clustering of parasite populations**

319 Expecting the changes in *kelch13* allele distributions to be a result of the change in prevalence of
320 circulating populations, we sought to examine population structure by clustering *Pf* barcodes by
321 similarity and examining the geographical distributions of the clusters. Clustering identical or near-
322 identical parasites (sharing at least 95% barcode similarity) identified 27 clusters with ≥20 members
323 (Table 1). In the period 2017-2019, four of the five largest clusters (KLV01, KLV02, KLV03 and KLV05),
324 accounting for 30% of samples (1,398/4,632), were found to carry both the *kelch13* C580Y mutation
325 and a *pm23* gene amplification, and thus likely to have emerged from the KEL1/PLA1 strain. Two of
326 these large clusters (KLV01 and KLV05) had considerable geographic spread across the eastern GMS
327 (Figure 6). Following the implementation of new frontline treatment policies, however, notable
328 changes occurred in the parasite populations. From 2020, clusters remained confined within single
329 countries, often restricted to single provinces, and populations of non-KEL1/PLA1 clusters began to
330 expand reaching high frequencies, as was the case for KLV04 and KLV07 in southern Laos and KLV12
331 in western Cambodia (Figure 6, Table 1). In Vietnam, the KEL1/PLA1-derived clusters KLV01 and KLV03
332 continued to circulate but lost their *pm23* amplification (Supplementary Table 4). By the third quarter
333 of 2021, none of the circulating clusters possessed the *pm23* amplification, and the Central Highlands
334 of Vietnam were dominated by the piperaquine-susceptible KLV03 population (Figure 6). Taken
335 together, these results suggest that the observed reduction in DHA-PPQ resistance in 2020-2021 can
336 be explained by the disappearance of KEL1/PLA1 clusters, or their loss of *pm23* amplification,
337 occurring after changes in first-line treatment policies.

338 **DISCUSSION**

339 In this study we analysed the genetic epidemiology of *Pf* in the eastern GMS through longitudinal
340 surveillance between 2017 and 2022, updating our previously published results.[9] Our data shows that
341 the revisions of first-line treatment policies in the region were followed by important changes in the
342 epidemiological landscape, which included: a marked decline in *Pf* infections, the near disappearance
343 of *pm23* amplifications and PPQ-R *crt* mutations from circulating strains, the fragmentation of the
344 artemisinin-resistant populations, and the absence of *mdr1* amplifications that would otherwise
345 threaten AS-MQ treatment efficacy.

346 The prevalence of DHA-PPQ resistant parasites collapsed from 62% in 2017-2019 to 1% in 2022, the
347 timing coinciding with the adoption of new first-line treatment strategies in three countries in the
348 eastern GMS. In the previous decade, the prolonged use of DHA-PPQ as frontline treatment resulted
349 in massive selective pressure on the parasites, and a rapid spread of KEL1/PLA1 lineages across the
350 eastern GMS.[12,13,42,43] The parasite population responded just as strikingly and rapidly to the release
351 of pressure from changes in treatment guidelines as it did to the intense DHA-PPQ pressure from
352 previous public health policies. It is likely that, in the absence of piperaquine pressure, *pm23*
353 amplifications and *crt* mutations associated with piperaquine resistance are costly in terms of parasite
354 fitness, and lead to a survival disadvantage in the absence of piperaquine pressure. A recent *in vitro*
355 study supported this notion by demonstrating that cultured C580Y parasites spontaneously de-amplify
356 *pm23* when piperaquine pressure is removed.[44] Thus, the change in policy appears to have produced
357 two different effects on KEL1/PLA1 parasites: either caused them to succumb in competition with
358 fitter ART-R strains, which previously had been circulating at low frequency alongside KEL1/PLA1;[37] or
359 cause them to de-amplify *pm23* while retaining their ART-R phenotype, improving their fitness under
360 the new circumstances.

361 The timeline of events also strongly suggests that the introduction of efficacious replacements for
362 DHA-PPQ, particularly in Vietnam, had a statistically significant impact, contributing to a rapid collapse

363 in the overall number of cases.[17,22-24] Similarly, *Pf* prevalence in Cambodia started to decline rapidly in
364 2018 (WHO data, Figure 1) following a change in treatment policy starting in 2017. Although our
365 dataset does not cover Cambodian samples from 2017-2019, evidence from other studies shows that
366 the KEL1/PLA1 population underwent sustained growth until 2018, constituting 75-100% of parasites
367 in multiple parts of Cambodia in 2016-2018.[13] Thus, the decline in Cambodia's prevalence during 2018-
368 2019, before any COVID-19-related movement restrictions, was not only rapid and geographically
369 widespread but also strain-specific, as the decline of KEL1/PLA1 give way to other ART-R strains. In the
370 southernmost provinces of Laos, the presence of KEL1/PLA1 parasites was most likely due to
371 importation from neighbouring regions of Cambodia or Thailand, where they circulated at high
372 frequency.[13,43] Although these ART-R parasite had been successful in Laos despite DHA-PPQ not being
373 the treatment of choice, their numbers declined as their frequencies waned in Cambodia and Thailand.
374 It is also likely that movement restrictions due to the pandemic would have made a major contribution
375 in reducing parasite importation, further accelerating the demise of KEL1/PLA1 in Laos and facilitating
376 the emergence of other ART-R strains.[37]

377 Reassuringly, we detected very few samples with predicted resistance to mefloquine, and none in
378 Cambodia where this drug is now used as part of the first-line ACT. On multiple occasions since the
379 1990s, the use of mefloquine has intermittently led to reduced treatment efficacy in the GMS, due to
380 the emergence of parasites possessing *mdr1* amplifications.[45] However, between 2019 and 2021 we
381 found only 9 isolates with *mdr1* amplifications, all in the province of Attapeu in Laos; seven of these
382 belonged to the *kelch13* R539T strain responsible for a *Pf* outbreak in 2021.[37] It is possible that this
383 amplification was under selection in that population because it confers somewhat reduced sensitivity
384 to lumefantrine, the partner drug in the frontline ACT of choice in Laos.[46,47] Our data showed a strong
385 association between the *mdr1* NFD haplotype (N86, Y184F, D1246) and the ART-R *kelch13* variants (in
386 particular C580Y, R539T, Y493H and C469F). Since this haplotype has been implicated in reducing
387 susceptibility to antimalarials including piperaquine[48] and mefloquine,[49] it is possible that it is under
388 selection due to its effect on partner drug response.

389 Although we can predict resistance for a broad range of antimalarials, a limitation to the current study
390 is the lack of validated genetic markers of resistance to a number of ACT partner drugs, including
391 pyronaridine, used in Thailand and Vietnam, and lumefantrine, used in Laos. Pyronaridine is a
392 relatively new drug, used only as a partner drug, for which no resistance has been detected to date; a
393 recent meta-analysis of 5,711 patients found that failure rates remain below 5%.[50] Lumefantrine, on
394 the other hand, is used in oral co-formulations with artemether as first-line treatment in most African
395 countries. While some studies have described phenotypic effects of *mdr1* variants, evidence is not
396 strong, and *mdr1*-induced reductions of *in vitro* susceptibility have not been reconciled with *in vivo*
397 clinical outcomes.[51,52] Further research, such as a highly statistically powered genome-wide
398 association study (GWAS), is needed to identify markers that can track resistance to these drugs, an
399 urgent matter in view of the recent emergence of artemisinin-resistant parasites in eastern Africa.[53]

400 Since GenRe-Mekong supports public health agencies, our protocols were designed to facilitate
401 integration with routine healthcare in low-resource settings, which demands some trade-off. As a
402 result, the present analysis is limited to symptomatic patients presenting at public health facilities,
403 and excludes asymptomatic infections. We also acknowledge there are gaps in our coverage, due to
404 differences in implementation schedules between countries, and a focus on the districts selected by
405 NMCPs as having the greatest relevance. In spite of these limitations, we have shown that continued
406 systematic routine surveillance with dense territory coverage is informative about epidemiological
407 changes and allows comparisons of prevalence between regions and over time. Monitoring genetic
408 markers allows efficient and rapid tracking of resistance, at a lower cost than therapeutic efficacy
409 studies.[54] As the GMS moves closer to elimination, and the number of infected *Pf* patients dwindle,
410 parasite populations will continue to change rapidly, and longitudinal surveillance will be an important
411 tool for supporting agile interventions. At the same time, surveillance planning will become
412 increasingly challenging, given the difficulty of predicting the smaller outbreaks that can be expected
413 in the elimination phase. In this epidemiological scenario, genetic surveillance will focus on use cases
414 relevant to sustained elimination and prevention of reintroduction, such as detection of imported

415 foreign malaria infections and outbreak analyses.[11,55] Furthermore, as *Pf* incidence diminishes, NMCPs
416 will have to control other *Plasmodium* species, notably *P. vivax*, for which very few surveillance tools
417 are currently available. GenRe-Mekong is committed to supporting NMCPs in the GMS with genetic
418 surveillance tools for *P. vivax*, currently under development.

419 One of the key challenges of genetic epidemiology is that of translating genetic data into actionable
420 knowledge relevant to NMCP activities, since mutations and haplotypes have little value without an
421 understandable context in which they can be assessed.[11] We developed the grcMalaria software
422 library with the aim of increasing the accessibility of genetic epidemiology analysis in daily practice,
423 simplifying and reducing time needed for analyses tasks. This freely available tool focuses on mapping,
424 using administrative divisions that are meaningful to NMCPs, and supporting flexible selection of
425 samples and division of the dataset into time slices, producing parallel maps for comparison. The
426 library incorporated clustering algorithms that group samples by similarity and map the distribution
427 of these clusters, allowing users to distinguish local strains from those spreading across borders.

428 The results presented in this study emphasize the importance of regional strategies for selection of
429 treatment policies to mitigate the spread of antimalarial drug resistance, and stresses the value of
430 selecting different first-line treatment regimens in neighboring countries. For future malaria
431 elimination efforts, genetic surveillance will support public health authorities, informing strategic
432 planning in the final phases of elimination.

433 **REFERENCES**

434 1 World Health Organization. World Malaria Report 2022. (2022).
435 <https://www.who.int/teams/global-malaria-programme/reports/world-malaria-report-
436 2022>.

437 2 Denis, M. B. *et al.* Efficacy of artemether-lumefantrine for the treatment of uncomplicated
438 *falciparum* malaria in northwest Cambodia. *Trop Med Int Health* **11**, 1800-1807 (2006).
439 https://doi.org/10.1111/j.1365-3156.2006.01739.x

440 3 Denis, M. B. *et al.* Surveillance of the efficacy of artesunate and mefloquine combination for
441 the treatment of uncomplicated falciparum malaria in Cambodia. *Trop Med Int Health* **11**,
442 1360-1366 (2006). https://doi.org/10.1111/j.1365-3156.2006.01690.x

443 4 van der Pluijm, R. W. *et al.* Determinants of dihydroartemisinin-piperaquine treatment failure
444 in *Plasmodium falciparum* malaria in Cambodia, Thailand, and Vietnam: a prospective clinical,
445 pharmacological, and genetic study. *Lancet Infect Dis* **19**, 952-961 (2019).
446 https://doi.org/10.1016/s1473-3099(19)30391-3

447 5 Mairet-Khedim, M. *et al.* Clinical and In Vitro Resistance of *Plasmodium falciparum* to
448 Artesunate-Amodiaquine in Cambodia. *Clin Infect Dis* **73**, 406-413 (2021).
449 https://doi.org/10.1093/cid/ciaa628

450 6 Plucinski, M. M. *et al.* Efficacy of artemether-lumefantrine, artesunate-amodiaquine, and
451 dihydroartemisinin-piperaquine for treatment of uncomplicated *Plasmodium falciparum*
452 malaria in Angola, 2015. *Malar J* **16**, 62 (2017). https://doi.org/10.1186/s12936-017-1712-4

453 7 Tumwebaze, P. K. *et al.* Decreased susceptibility of *Plasmodium falciparum* to both
454 dihydroartemisinin and lumefantrine in northern Uganda. *Nat Commun* **13**, 6353 (2022).
455 https://doi.org/10.1038/s41467-022-33873-x

456 8 Dondorp, A. M. *et al.* Artemisinin resistance in *Plasmodium falciparum* malaria. *N Engl J Med*
457 **361**, 455-467 (2009).

458 9 Jacob, C. G. *et al.* Genetic surveillance in the Greater Mekong subregion and South Asia to
459 support malaria control and elimination. *Elife* **10** (2021). https://doi.org/10.7554/eLife.62997

460 10 Mayor, A. *et al.* Prospective surveillance study to detect antimalarial drug resistance, gene
461 deletions of diagnostic relevance and genetic diversity of *Plasmodium falciparum* in
462 Mozambique: protocol. *BMJ Open* **12**, e063456 (2022). https://doi.org/10.1136/bmjopen-
463 2022-063456

464 11 Miotto, O. Genetic Epidemiology Use Cases for Malaria Control Programmes: A Methodology.
465 (2023). <https://www.malariagen.net/resource/genetic-epidemiology-use-cases-malaria-
466 control-programmes-methodology/>.

467 12 Amato, R. *et al.* Genetic markers associated with dihydroartemisinin-piperaquine failure in
468 *Plasmodium falciparum* malaria in Cambodia: a genotype-phenotype association study.
469 *Lancet Infect Dis* **17**, 164-173 (2017). https://doi.org/10.1016/s1473-3099(16)30409-1

470 13 Hamilton, W. L. *et al.* Evolution and expansion of multidrug-resistant malaria in southeast Asia:
471 a genomic epidemiology study. *Lancet Infect Dis* **19**, 943-951 (2019).
472 https://doi.org/10.1016/s1473-3099(19)30392-5

14 World Health Organization. Guidelines for the treatment of malaria. (2015). <https://iris.who.int/handle/10665/162441>.

15 Amaratunga, C. *et al.* Dihydroartemisinin-piperaquine resistance in *Plasmodium falciparum* malaria in Cambodia: a multisite prospective cohort study. *The Lancet. Infectious diseases* **16**, 357-365 (2016). https://doi.org/10.1016/S1473-3099(15)00487-9

16 World Health Organization. The Mekong Malaria Elimination programme. Accelerating malaria elimination in the Greater Mekong. (2022). <https://www.who.int/publications/i/item/WHO-UCN-GMP-MME-2022.01>.

17 Cambodia: National Center for Parasitology, E. a. M. C. C. National Center for Parasitology, Entomology and Malaria Control: National Malaria Programme Review 2019. (2019).

18 Peto, T. J. *et al.* Triple therapy with artemether-lumefantrine plus amodiaquine versus artemether-lumefantrine alone for artemisinin-resistant, uncomplicated falciparum malaria: an open-label, randomised, multicentre trial. *Lancet Infect Dis* **22**, 867-878 (2022). https://doi.org/10.1016/S1473-3099(21)00692-7

19 Imwong, M. *et al.* Evolution of Multidrug Resistance in *Plasmodium falciparum*: a Longitudinal Study of Genetic Resistance Markers in the Greater Mekong Subregion. *Antimicrob Agents Chemother* **65**, e0112121 (2021). https://doi.org/10.1128/AAC.01121-21

20 Vietnam Ministry of Health. National Guideline of Malaria Diagnosis and Treatment. (Hanoi, 2020).

21 Cao, V. A. T. *et al.* Exploring the feasibility of introducing triple artemisinin-based combination therapy in the malaria treatment policy in Vietnam. *Malaria Journal* **22**, 326 (2023). https://doi.org/10.1186/s12936-023-04763-4

22 World Health Organizaion. Mekong malaria elimination programme: Accelerating malaria elimination in the Greater Mekong, bulletin 10. (2022).

23 Sudathip, P. *et al.* Progress and challenges of integrated drug efficacy surveillance for uncomplicated malaria in Thailand. *Malar J* **20**, 261 (2021). https://doi.org/10.1186/s12936-021-03791-2

24 Simmalavong, N. *et al.* Expanding malaria diagnosis and treatment in Lao PDR: lessons learned from a public-private mix initiative. *Malar J* **16**, 460 (2017). https://doi.org/10.1186/s12936-017-2104-5

25 Daniels, R. F. *et al.* Modeling malaria genomics reveals transmission decline and rebound in Senegal. *Proc Natl Acad Sci U S A* **112**, 7067-7072 (2015). https://doi.org/10.1073/pnas.1505691112

26 Wong, W. *et al.* R (H): a genetic metric for measuring intrahost *Plasmodium falciparum* relatedness and distinguishing cotransmission from superinfection. *PNAS Nexus* **1**, pgac187 (2022). https://doi.org/10.1093/pnasnexus/pgac187

27 Kattenberg, J. H. *et al.* Novel highly-multiplexed AmpliSeq targeted assay for Plasmodium vivax genetic surveillance use cases at multiple geographical scales. *Front Cell Infect Microbiol* **12**, 953187 (2022). https://doi.org/10.3389/fcimb.2022.953187

28 R Core Team (2021). R: A language and environment for statistical computing. R Foundation for Statistical Computing, V., Austria. URL https://www.R-project.org/.

29 Areas, G. A. *GADM database of Global Administrative Areas, version 2.0. [online] URL: www.gadm.org.*, 2012).

30 MalariaGen *et al.* Pf7: an open dataset of *Plasmodium falciparum* genome variation in 20,000 worldwide samples. *Wellcome Open Res* **8**, 22 (2023). https://doi.org/10.12688/wellcomeopenres.18681.1

31 World Health Organizaion. Mekong malaria elimination programme: epidemiology summary, volume 4, October-December 2018. (2018).

32 World Health Organizaion. Mekong malaria elimination programme: epidemiology summary, volume 12, October-December 2020. (World Health Organisation 2020).

33 World Health Organizaion. Mekong malaria elimination programme: epidemiology summary, volume 20, October–December 2022. (World Health Organisation 2023).

34 Global Malaria Programme (GMP). Report on antimalarial drug efficacy, resistance and response: 10 years of surveillance (2010-2019). (World Health Organisation, 2020).

35 H, W. Wickham H (2016). ggplot2: Elegant Graphics for Data Analysis. Springer-Verlag New York. ISBN 978-3-319-24277-4, https://ggplot2.tidyverse.org. (2016).

36 A, S. DescTools: Tools for Descriptive Statistics. R package version 0.99.54, https://andrisignorell.github.io/DescTools/. (2024).

37 Wasakul, V. *et al.* Malaria outbreak in Laos driven by a selective sweep for *Plasmodium falciparum kelch13* R539T mutants: a genetic epidemiology analysis. *The Lancet Infectious Diseases* **23**, 568-577 (2023). https://doi.org/10.1016/S1473-3099(22)00697-1

38 Blondel, V. D., Guillaume, J.-L., Lambiotte, R. & Lefebvre, E. Fast unfolding of communities in large networks. *Journal of Statistical Mechanics: Theory and Experiment* **2008**, P10008 (2008). https://doi.org/10.1088/1742-5468/2008/10/P10008

39 Price, R. N. *et al.* Mefloquine resistance in *Plasmodium falciparum* and increased pfmdr1 gene copy number. *Lancet* **364**, 438-447 (2004). https://doi.org/10.1016/S0140-6736(04)16767-6

40 Miotto, O. *et al.* Multiple populations of artemisinin-resistant *Plasmodium falciparum* in Cambodia. *Nature Genetics* **45**, 648-655 (2013). https://doi.org/10.1038/ng.2624

41 Miotto, O. *et al.* Genetic architecture of artemisinin-resistant *Plasmodium falciparum*. *Nat Genet* **47**, 226-234 (2015). https://doi.org/10.1038/ng.3189

42 Imwong, M. *et al.* Molecular epidemiology of resistance to antimalarial drugs in the Greater Mekong subregion: an observational study. *Lancet Infect Dis* **20**, 1470-1480 (2020). https://doi.org/10.1016/S1473-3099(20)30228-0

43 Imwong, M. *et al.* The spread of artemisinin-resistant *Plasmodium falciparum* in the Greater Mekong subregion: a molecular epidemiology observational study. *Lancet Infect Dis* **17**, 491-497 (2017). https://doi.org/10.1016/S1473-3099(17)30048-8

44 Mok, S. *et al.* Mapping the genomic landscape of multidrug resistance in *Plasmodium falciparum* and its impact on parasite fitness. *Sci Adv* **9**, eadi2364 (2023). https://doi.org/10.1126/sciadv.adi2364

552 45 Lek, D. *et al.* Efficacy of three anti-malarial regimens for uncomplicated *Plasmodium*
553 *falciparum* malaria in Cambodia, 2009-2011: a randomized controlled trial and brief review.
554 *Malar J* **21**, 259 (2022). https://doi.org/10.1186/s12936-022-04279-3

555 46 Price, R. N. *et al.* Molecular and pharmacological determinants of the therapeutic response to
556 artemether-lumefantrine in multidrug-resistant *Plasmodium falciparum* malaria. *Clin Infect*
557 *Dis* **42**, 1570-1577 (2006). https://doi.org/10.1086/503423

558 47 Sidhu, A. B. *et al.* Decreasing pfmdr1 copy number in *plasmodium falciparum* malaria
559 heightens susceptibility to mefloquine, lumefantrine, halofantrine, quinine, and artemisinin. *J*
560 *Infect Dis* **194**, 528-535 (2006). https://doi.org/10.1086/507115

561 48 Veiga, M. I. *et al.* Globally prevalent PfMDR1 mutations modulate *Plasmodium falciparum*
562 susceptibility to artemisinin-based combination therapies. *Nature Communications* **7**, 11553
563 (2016). https://doi.org/10.1038/ncomms11553

564 49 Sisowath, C. *et al.* The role of pfmdr1 in *Plasmodium falciparum* tolerance to artemether-
565 lumefantrine in Africa. (2007).

566 50 Pryce, J., Taylor, M., Fox, T. & Hine, P. Pyronaridine-artesunate for treating uncomplicated
567 *Plasmodium falciparum* malaria. *Cochrane Database Syst Rev* **6**, CD006404 (2022).
568 https://doi.org/10.1002/14651858.CD006404.pub4

569 51 Lim, P. *et al.* Pfmdr1 copy number and arteminisin derivatives combination therapy failure in
570 falciparum malaria in Cambodia. *Malar J* **8**, 11 (2009). https://doi.org/10.1186/1475-2875-8-
571 11

572 52 Baraka, V. *et al.* Impact of treatment and re-treatment with artemether-lumefantrine and
573 artesunate-amodiaquine on selection of *Plasmodium falciparum* multidrug resistance gene-1
574 polymorphisms in the Democratic Republic of Congo and Uganda. *PLoS One* **13**, e0191922
575 (2018). https://doi.org/10.1371/journal.pone.0191922

576 53 Rosenthal, P. J. *et al.* The emergence of artemisinin partial resistance in Africa: how do we
577 respond? *Lancet Infect Dis* (2024). https://doi.org/10.1016/S1473-3099(24)00141-5

578 54 Nsanzabana, C. *et al.* Molecular assays for antimalarial drug resistance surveillance: A target
579 product profile. *PLOS ONE* **13** (2018). https://doi.org/ e0204347

580 55 Noviyanti, R. *et al.* Implementing parasite genotyping into national surveillance frameworks:
581 Feedback from control programmes and researchers in the Asia-Pacific region. *Malaria*
582 *Journal* **19**, 1-20 (2020). https://doi.org/10.1186/s12936-020-03330-5

583

584 **ACKNOWLEDGEMENTS**

585 This study was funded by the Bill & Melinda Gates Foundation (grant numbers OPP11188166,
586 OPP1204628, INV-001927) and by The Global Fund to Fight AIDS, Tuberculosis and Malaria (grant
587 number QSE-M-UNOPS-MORU-20864-007-44). This research was funded in part by the Wellcome
588 Trust (grant number 204911). The authors wish to thank all the patients and guardians who generously
589 agreed to provide blood samples, and all public health and medical staff who participated in the
590 collection of those samples. Genome sequencing and genotyping was performed by the WSI and
591 OUCRU, and sequencing data processing was supported by the MalariaGEN Resource Centre. We
592 thank the staff of the WSI Sample Logistics, Sequencing, and Informatics facilities for their
593 contribution; Eleanor Drury for support in the sample processing pipeline.

594 **AUTHOR CONTRIBUTIONS**

595 V.W., T.D.V. and O.M. conceived and designed the study. N.T-N., H.H.Q., N.D.T., K.C., S.S., S.M., V.B.,
596 V.S., M.M., N.T.K.T., V.N.L.P., S.C., S.P., and S.X. coordinated sample and data collection. P.D.T., N.T-
597 N., S.G., R.D.P., and C.V.A. processed samples, and generated genomic data. V.W., T.D.V., E.B., and
598 O.M. developed methods, analysed and interpreted data. V.J.S., P.N.N., E.A.A., R.J.M., N.P.D., A.M.D.,
599 and O.M. managed and coordinated the genetic surveillance project. V.W., T.D.V., E.B., and O.M.
600 wrote and revised the manuscript. V.W., T.D.V. and O.M. accessed and verified all the data. All authors
601 provided critical revision of the manuscript. All authors had full access to all the data in the study and
602 had final responsibility for the decision to submit for publication.

603 **COMPETING INTERESTS**

604 The authors have no competing interests to declare.

605

606 **TABLES AND FIGURES**

607 **Table 1. Temporal distribution of *P. falciparum* sample clusters.** For each cluster, we show: the
608 cluster label; the name by which the cluster was identified in previous studies, if any; in each year of
609 collection, the proportion of samples that belong to the cluster; the proportion of samples predicted
610 resistant to artemisinin (ART), piperaquine (PPQ), and mefloquine (MQ), chloroquine (CQ), sulfadoxine
611 (SX) and pyrimethamine (PM); the majority *kelch13* variant carried by parasites in the cluster; and
612 whether the cluster carries a KEL1/PLA1 haplotype. Only clusters with ≥20 members are shown; the
613 full list of clusters can be found at Supplementary Table 5. Samples that were not assigned to a cluster
614 with these parameters were labelled as 'not clustered'.

		Proportion of samples in each year						Resistance							
Cluster	**Previous names**	**2017**	**2018**	**2019**	**2020**	**2021**	**2022**	**ART**	**PPQ**	**MQ**	**CQ**	**SX**	**PM**	**Main *kelch13***	**KEL1/PLA1**
KLV01		5%	8%	21%	16%	4%		100%	89%	0%	100%	100%	100%	C580Y	Yes
KLV02		1%	12%	18%	4%			100%	98%	0%	100%	100%	100%	C580Y	Yes
KLV03			1%	13%	10%	16%	33%	100%	54%	0%	100%	100%	100%	C580Y	Yes
KLV04	LAA1[a]	0%	0%	0%	18%	15%	4%	100%	0%	13%	100%	100%	100%	R539T	
KLV05		4%	4%	3%	3%	0%		100%	78%	0%	100%	100%	100%	C580Y	Yes
KLV06		5%	3%	1%	1%			6%	1%	0%	100%	0%	100%	WT	
KLV07	LAA2[a]; KH2[b]	1%	1%	0%	3%	10%	9%	100%	1%	0%	100%	100%	100%	C580Y	
KLV08		5%	2%	0%				100%	84%	0%	100%	100%	100%	C580Y	Yes
KLV09		1%	1%	3%	4%			100%	100%	0%	100%	100%	100%	C580Y	Yes
KLV10		3%	2%	0%	0%			1%	0%	0%	100%	0%	100%	WT	
KLV11				0%		14%		0%	0%	0%	0%	0%	100%	WT	
KLV12						1%	16%	100%	0%	0%	100%	100%	100%	Y493H	
KLV13		2%	1%	1%				0%	2%	0%	100%	100%	100%	WT	
KLV14		0%	1%	2%	1%			100%	85%	0%	100%	100%	100%	C580Y	Yes
KLV15			2%	0%	0%			0%	0%	0%	100%	100%	100%	WT	
KLV16		1%	1%			0%		8%	0%	0%	100%	0%	100%	WT	
KLV17			1%	0%	3%			0%	0%	0%	100%	0%	100%	WT	
KLV18		2%	1%	0%				100%	97%	0%	100%	100%	100%	C580Y	Yes
KLV19		0%	1%	0%				0%	0%	0%	100%	0%	100%	WT	
KLV20			1%		0%			0%	0%	0%	100%	0%	100%	WT	
KLV21			1%	0%				0%	0%	0%	100%	100%	100%	WT	
KLV22		1%	0%	1%				0%	0%	0%	100%	100%	100%	WT	
KLV23					1%	4%	1%	100%	0%	0%	100%	100%	100%	C580Y	
KLV24		1%	1%					100%	100%	0%	100%	100%	100%	C580Y	Yes
KLV25		1%	1%	0%				75%	0%	0%	100%	100%	100%	C580Y	
KLV26		0%		1%	1%			100%	94%	0%	100%	100%	100%	C580Y	Yes
KLV27		1%	0%	0%				0%	7%	0%	100%	100%	100%	WT	
Not clustered		55%	43%	30%	26%	26%	36%								
Total samples		1291	1894	1447	608	413	329								

615 [a] Wasakul, et al. [37]
616 [b] Miotto, et al. [40]
617

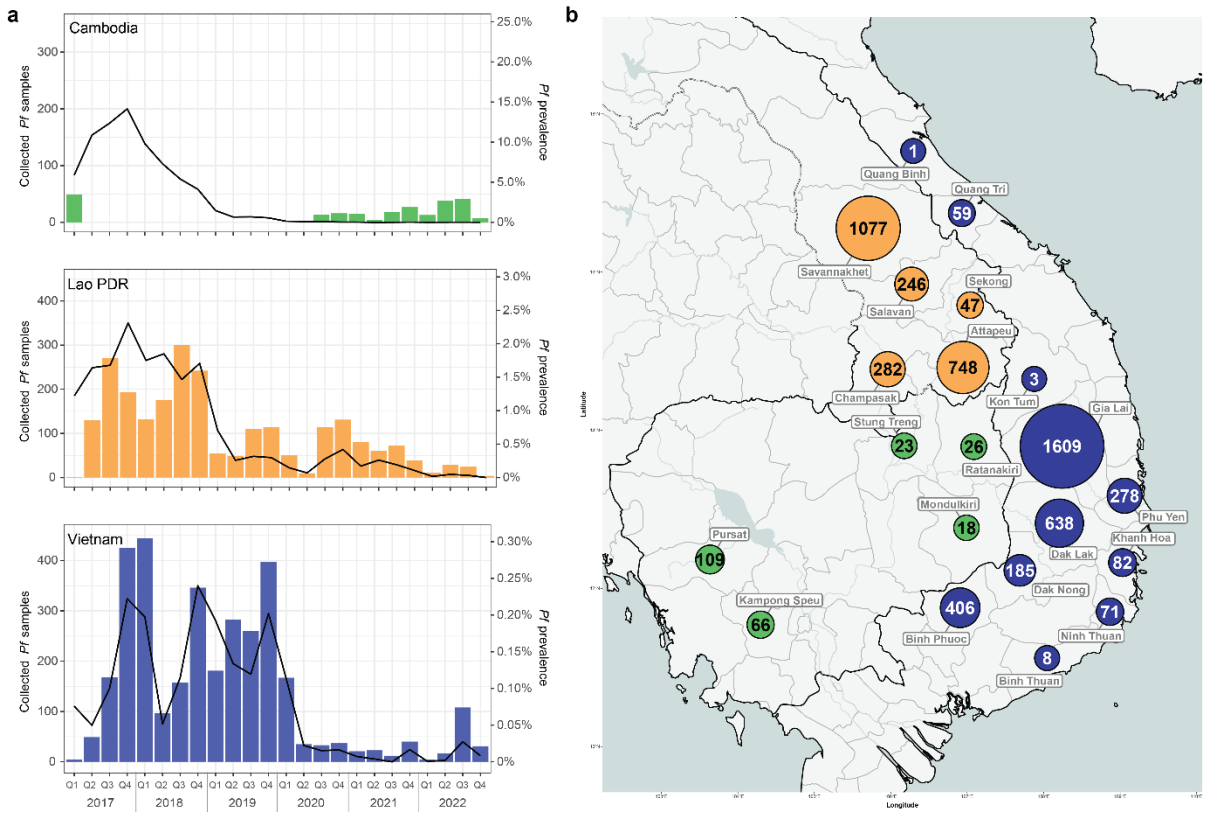

Figure 1. *P. falciparum* (*Pf*) samples genotyped by GenRe-Mekong during the study period. **a** Quarterly counts of *Pf* samples collected and genotyped by the GenRe-Mekong project, presented as bar charts. No routine surveillance was carried out by GenRe-Mekong in Cambodia in 2018 and 2019. Malaria prevalence, calculated as the proportion of confirmed *Pf* cases over the total number of tested cases, as reported by WHO,[31-33] is shown as a black line in each chart. The prevalence scales differ between countries. **b** Spatial distributions by province of *Pf* samples collected between 2017 and 2022. Markers are coloured by country, and marker size is proportional to sample size.

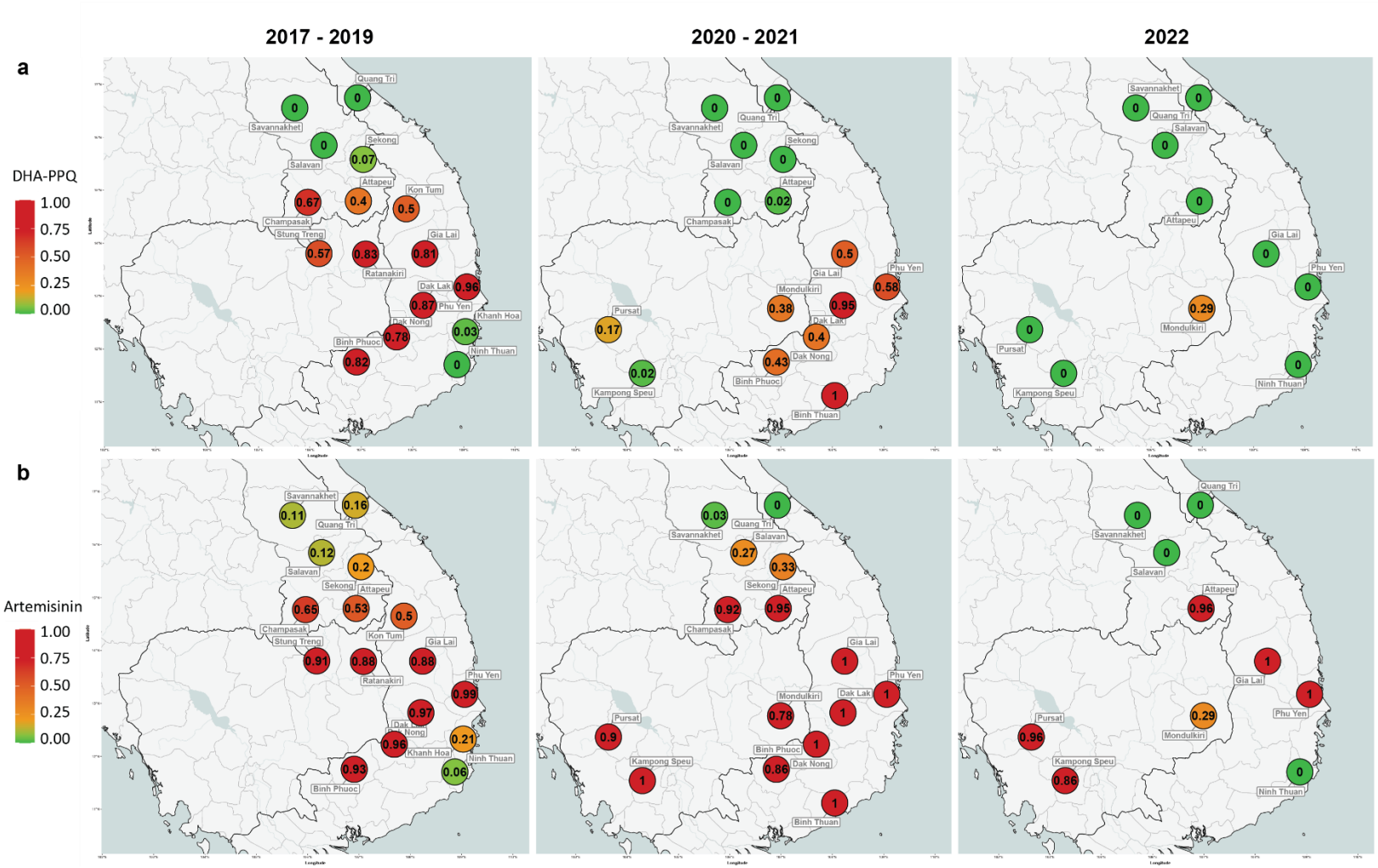

Figure 2. Predicted resistance to a) dihydroartemisinin-piperaquine (DHA-PPQ) and b) artemisinin at provincial level. Left: 2017-2019, middle: 2020-2021, right: January – December 2022. Resistance was predicted based on a published set of phenotype rules (Supplementary Table 1).[9] Marker colours reflects resistance prevalence, ranging from 0 to 1, where 0 means no parasites were predicted to be resistant, and 1 means 100% of the parasites in the province carried the relevant resistance markers. A marker appears when at least 2 samples were processed from the province.

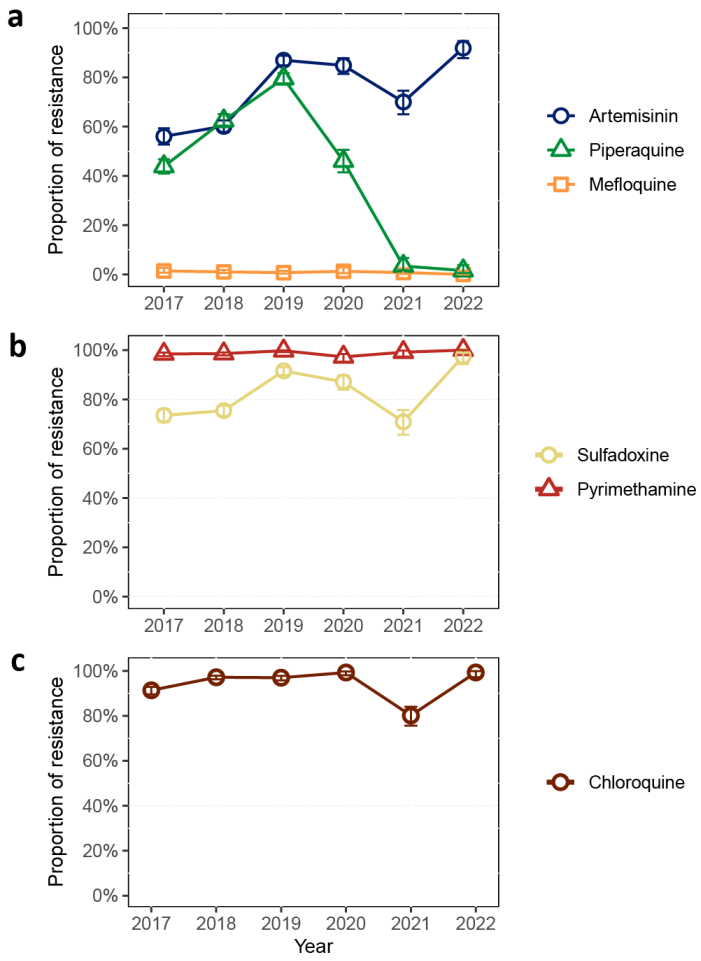

Figure 3. Predicted regional antimalarial resistance from 2017 to 2022. Panels show the trend in proportions of samples predicted to be resistant to **a** artemisinin, piperaquine and mefloquine, **b** sulfadoxine and pyrimethamine and **c** chloroquine. Error bars indicate 95% confidence intervals.

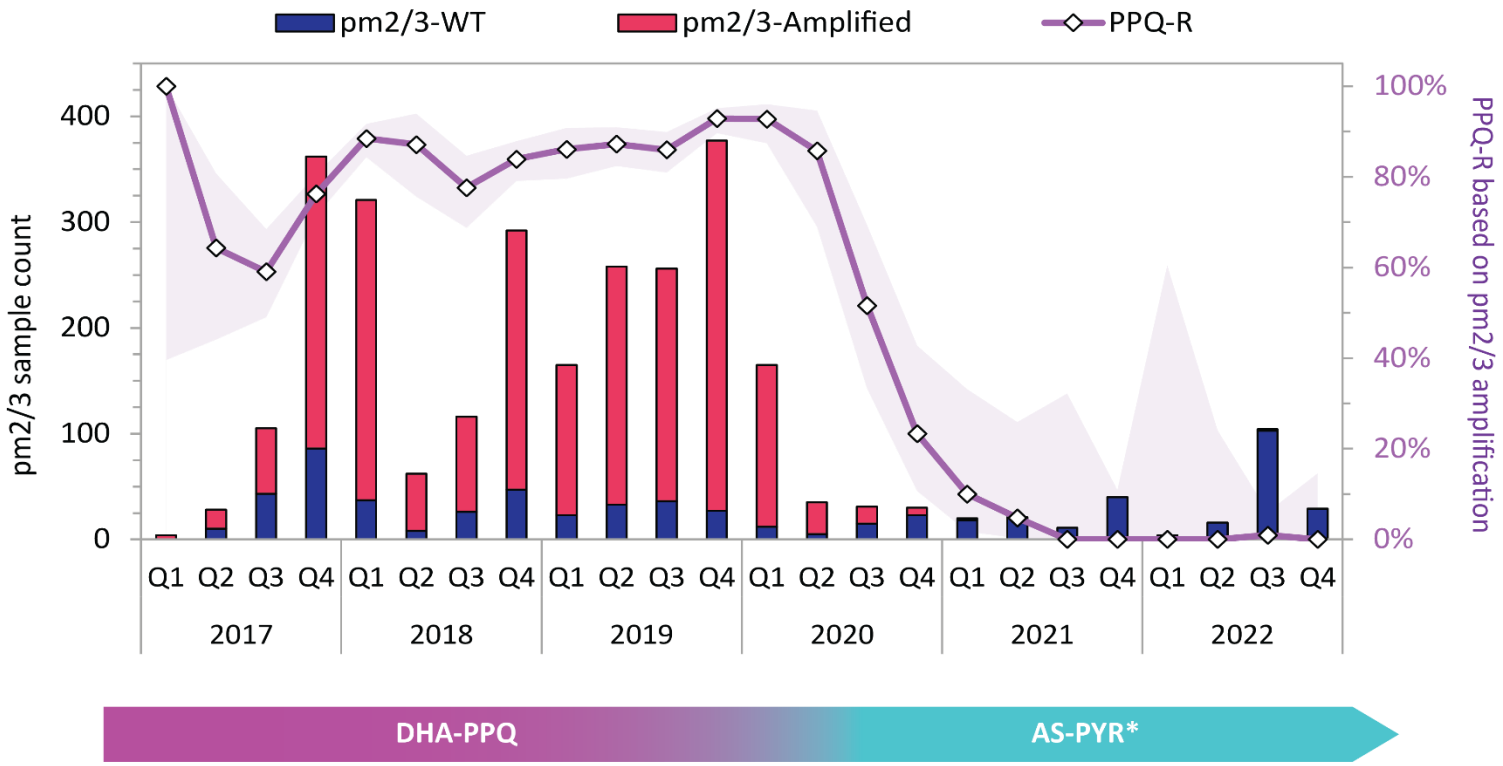

Figure 4. Predicted levels of piperaquine resistance in five endemic provinces of Vietnam. The bar chart shows the quarterly numbers of samples (left axis) with wild-type (WT, navy) and *plasmepsin2/3* gene amplification (red), against the proportion of piperaquine resistance (PPQ-R) samples in five endemic provinces in Vietnam (right axis). Purple shaded area shows 95% confidence interval of the PPQ-R proportion estimate. Q1: January-March; Q2: April-June; Q3: July-September; Q4: October-December. The bar below the graph shows first-line treatment policy for uncomplicated *P. falciparum* in Vietnam, showing the timeline of transition from dihydroartemisinin-piperaquine (DHA-PPQ) to pyronaridine-artesunate (AS-PYR). *AS-PYR was adopted in 5 endemic provinces (Binh Phuoc, Dak Nong, Gia Lai, Dak Lak, and Phu Yen) [20,21].

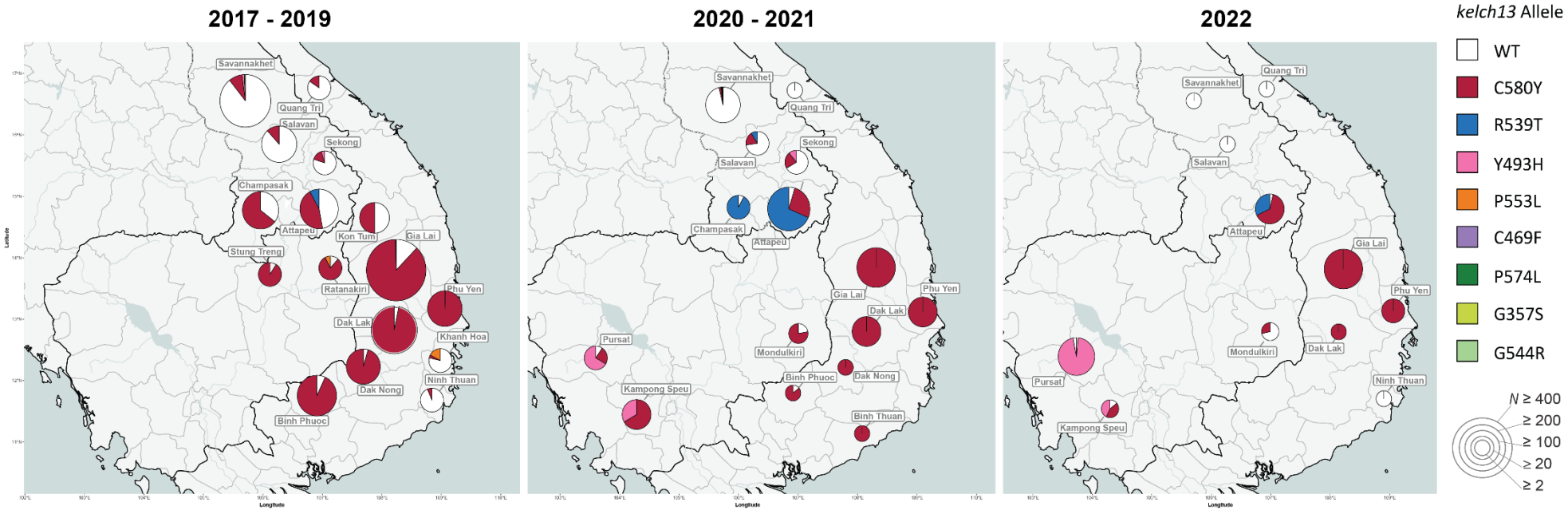

Figure 5. Prevalence of *kelch13* alleles between 2017 and 2022. The pie chart shows the proportions of *kelch13* alleles in each province where samples were collected. Pie chart size represents the number of samples from the province (*N*). Wild-type (WT) parasites are predicted to be sensitive to artemisinin. All but two of the *kelch13* alleles detected in this study have been associated with delayed parasite clearance, and thus predictive of artemisinin resistance. Since the two rare alleles G357S and G544R are not in World Health Organization's validated marker list, their association with artemisinin resistance is undetermined.

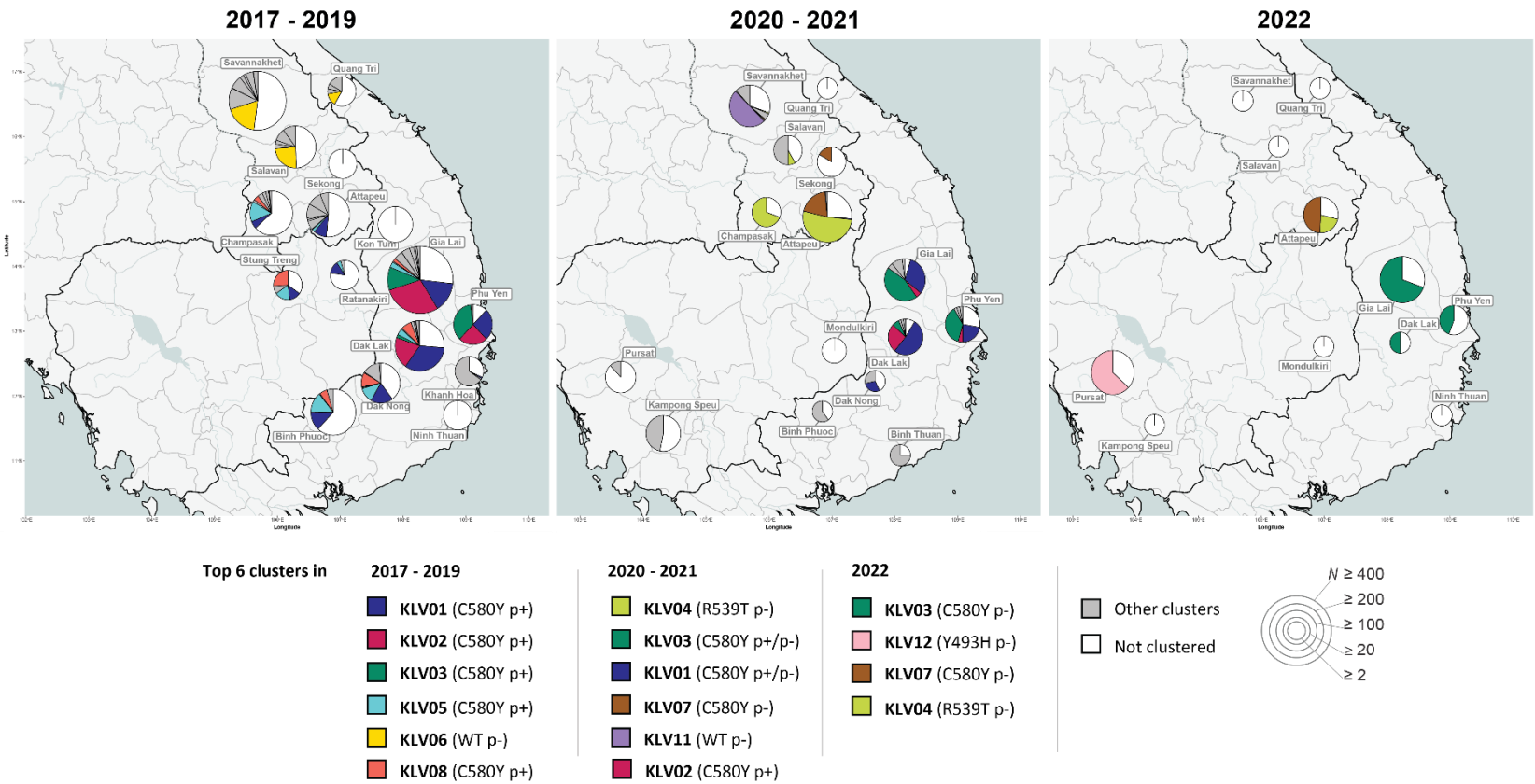

Figure 6. Proportion of the most prevalent *P. falciparum* clusters in each province across three periods. Left panel: 2017-2019, middle: 2020-2021, right: January-December 2022. Clusters were identified by applying community detection algorithm to a graph of parasites sharing at least 95% genetic barcode identity, identifying 64 clusters with at least 10 members. In 2017-2019, 54 clusters were present, while 14 clusters were present in 2020-2021 and only four clusters were found in 2022. Pie chart size represents the sample size for the province (*N*). To improve visualization, the top six clusters in each period were assigned colours, while the remaining smaller clusters are shown in gray. White segments represent the proportions of samples that were not assigned to a cluster. In the legend, clusters are arranged in descending order of cluster size for each period. The main *kelch13* variant observed in the cluster and a label denoting *plasmepsin2/3* amplification (p+) or *plasmepsin2/3* wild-type (p-), are shown in brackets following the cluster name.